

Nanoindentation study of light-induced softening of  
supramolecular and covalently functionalized azo  
polymers

Cite this: DOI: 10.1039/c3tc30246f

Received 6th February 2013  
Accepted 8th March 2013

DOI: 10.1039/c3tc30246f

www.rsc.org/MaterialsC

Jaana Vapaavuori,<sup>†a</sup> Zahid Mahimwalla,<sup>†b</sup> Richard R. Chromik,<sup>c</sup> Matti Kaivola,<sup>a</sup>  
Arri Priimagi<sup>\*a</sup> and Christopher J. Barrett<sup>\*b</sup>

Nanoindentation studies on thin films of the widely used azo polymer pDR1A and a supramolecular polymer–azobenzene complex p4VP(DY7)<sub>0.5</sub> demonstrate significant light-induced softening upon visible-light irradiation due to *trans*–*cis*–*trans* photoisomerization of the azobenzene units. More specifically, the strain-rate sensitivities of pDR1A and p4VP(DY7)<sub>0.5</sub> upon 532 nm irradiation increase by 80% and 120%, respectively. These results imply a photosoftening contribution to the mechanisms of light-induced surface patterning of azo polymers and the photomechanical effect. The finding that under the experimental conditions used photosoftening is more significant in the supramolecular complex than in the covalently functionalized polymer highlights the potential of noncovalent functionalization strategies in designing materials with efficient photomechanical response, and nanoindentation provides a powerful technique to quantify the connection between the photoinduced changes in mechanical properties and photoinduced macroscopic movement of azo polymer films.

Azobenzene-containing materials have received much recent interest for their ability to actuate with light photo-mechanically, and to undergo micron-scale mass transport upon irradiation with non-uniform light field or interference pattern.<sup>1</sup> The origin of these fascinating photomechanical effects is still under investigation, but is clearly a consequence of *trans*–*cis*–*trans* photoisomerization of azobenzene upon irradiation, which can for instance give rise to high-modulation-depth surface patterns. Such surface patterns have been applied, *e.g.*, in soft lithography and replica molding,<sup>2</sup> photochemical imaging,<sup>3</sup> and direct nanofabrication.<sup>4</sup> However, despite extensive research since the discovery of the phenomenon in 1995,<sup>1</sup> a

complete understanding of the underlying mechanism has not yet been achieved, although a significant photoinduced change in modulus and/or viscosity has been strongly implicated, and is practically requisite for achieving such light-induced flow at room temperature of glassy systems. In order to rationally design photo-deformable or photo-mechanical material systems with optimized performance, it is imperative to understand the light-induced changes of the mechanical material properties. This knowledge may also significantly contribute to fundamental understanding of light–matter interactions in azobenzene-based materials.

Efforts towards understanding the surface-pattern formation have focused either on explaining the nature of the driving force,<sup>5</sup> or modelling the viscoelastic flow of the polymeric material during the pattern formation.<sup>6</sup> In general however, successful models describing this viscoelastic flow assume that the viscosity of the polymeric material is reduced from its bulk value close to the value of the molten polymer under light illumination.<sup>6c,d</sup> It has been shown that the temperature rise at the intensity levels typically used in the grating inscription is only in the range of few Kelvins at most,<sup>7</sup> and also that heating of the sample above the glass transition temperature can erase the formed patterns such as surface relief gratings (SRGs) in most amorphous azo polymer systems. These observations then suggest a photo-induced origin of the required viscosity decrease. Indeed, photoinduced changes in the mechanical properties (*e.g.* softening of the material) of azo-polymer thin films upon light irradiation have been studied *via* several experiments. Among the first quantitative studies on the topic in 2000, Srikhirin and Neher *et al.* reported that azobenzene-doped polymers tend to soften upon irradiation with visible light,<sup>8</sup> due to continuous *trans*–*cis*–*trans* cycling of the azobenzene units. On the other hand, UV irradiation (which drives the molecules from *trans*- to *cis*-form) appeared to harden the material. Later in 2005, a similar observation from the same group was made in azobenzene-functionalized side-chain polymers.<sup>9</sup> However, the light-induced softening in these systems was shown to be minor compared to the case of heating

<sup>a</sup>Department of Applied Physics, Aalto University, P.O. Box 13500, 00076 Aalto, Finland. E-mail: arri.priimagi@aalto.fi

<sup>b</sup>Department of Chemistry, McGill University, Montreal, QC, H3A 2K6, Canada. E-mail: christopher.barrett@mcgill.ca

<sup>c</sup>Department of Mining and Materials Engineering, McGill University, 3610 University Street, Montreal, QC, H3A 0C5, Canada

† These authors contributed equally to this work.

the polymer film in the dark.<sup>10</sup> In crosslinked azobenzene-containing amorphous and liquid-crystalline polymer networks, UV irradiation has been reported to decrease the elastic modulus, *i.e.*, to soften the material system, in contrast to the non-crosslinked systems previously reported.<sup>11</sup>

Perhaps the most ambitious study undertaken to date has been carried out by Karageorgiev and Neher *et al.* who estimated photoinduced changes of viscoelastic behaviour for the widely used covalently functionalized pDR1M polymer using load-penetration curves from AFM-based indentation experiments.<sup>12</sup> They reported a 74% decrease in elastic modulus upon visible-light irradiation, and a more pronounced photo-induced change in viscosity of many orders of magnitude. They also clearly distinguished between light- and heat-induced processes by showing that irradiation with linearly polarized light leads to directional viscoelastic flow parallel to the light polarization. This work has recently been used as a basis for a nano-structuring technique termed directional photofluidization lithography.<sup>4b</sup> These previous reports of various materials studied by various techniques suggest that light-induced changes of mechanical properties vary strongly with structural details of the azobenzene-containing material systems in question. It is also noteworthy that *supramolecular polymer-azobenzene complexes*, which have in recent years emerged as one of the most efficient SRG-forming materials,<sup>13</sup> had not been included in any such studies. As the complexation is based on spontaneous non-covalent interactions, such materials allow for easy control over, for *e.g.*, the concentration of the photoactive units and the molecular weight of the host polymer, both of which significantly affect the SRG formation in azo polymers. At the same time, the SRG formation efficiency is not compromised with respect to covalently functionalized polymers, rendering supramolecular materials promising from the viewpoint of both fundamental and applied studies.

Alongside AFM, depth-sensing nanoindentation provides an excellent tool to characterize the mechanical properties of soft materials, with the possibility to study surface phenomena such as SRG formation with high accuracy in the thickness range of hundreds of nanometers. The clear advantage of nanoindentation with respect to AFM is that modelling of the tip shape and independent measurement of the cantilever spring constant are not required.<sup>14</sup> Indeed, very interesting results of the photoplasticity of chalcogenide glasses,<sup>15</sup> and strain-rate sensitivity and creep of polymeric materials have been shown by nanoindentation.<sup>16</sup> Scattered examples of using nanoindentation in context of azo polymers also exist: Moniruzzaman and co-workers have observed that the stiffness of azobenzene-containing side-chain copolymers increases upon UV irradiation.<sup>17</sup> Richter and co-workers took an effort to study the mechanical properties of the crests and troughs of an SRG *via* nanoindentation, also reporting increased elastic modulus and hardness immediately after irradiation.<sup>18</sup>

In this work, we perform nanoindentation studies of the photo-induced changes in mechanical properties of a hydrogen-bonded polymer-azobenzene complex, p4VP(DY7)<sub>0.5</sub>,<sup>19</sup> and the widely studied covalently functionalized azo-polymer pDR1A (Fig. 1). The former has recently proven to be an efficient

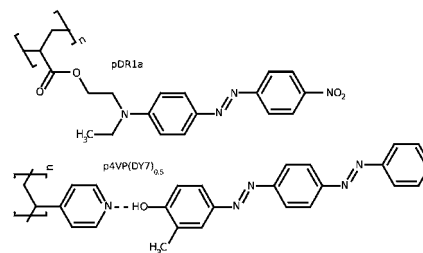


Fig. 1 Chemical structures of the supramolecular complex p4VP(DY7)<sub>0.5</sub> and the covalently functionalized pDR1A.

material for SRG formation even though (i) the chromophore DY7 is non-polar, and (ii) its absorption at the visible wavelength range used to inscribe the gratings is quite small.<sup>19b</sup> Based on the load-depth curves both in dark and under light illumination, the strain-rate sensitivities<sup>20</sup> of these two materials are calculated and compared. The main finding of this work is that the supramolecular complex based on the nonpolar DY7 dye leads to more pronounced photo-softening than the conventional and efficient (in terms of SRG formation) DR1-based acrylate. We also clearly demonstrate the power of the nanoindentation technique on gaining important information on the photoresponsive behaviour of azobenzene-based materials.

To compare the photoinduced changes in the mechanical properties of the materials under investigation, we follow the determination of the strain-rate sensitivity, *m*, introduced by Mayo and Nix:<sup>20</sup>

$$m = \left( \frac{d[\log \sigma]}{d[\log \dot{\epsilon}]} \right) \quad (1)$$

Experimentally, the strain-rate sensitivity can be determined by measuring the strain-rate,  $\dot{\epsilon}$ , at certain value of the stress,  $\sigma$ , (this case at constant depth) and by varying the loading rates. The stress is defined by  $\sigma = P/A$ , where *P* equals the applied loading force, and the projected contact area *A* at the depth *h* is calculated by

$$A = C_0 h^2 + C_1 h + C_2 h^{\frac{1}{2}} + C_3 h^{\frac{1}{4}} \quad (2)$$

where the constants  $C_0 - C_3$  depend on the tip geometry. Strain-rate  $\dot{\epsilon}$  can be written in the form

$$\dot{\epsilon} = \left( \frac{1}{h} \right) \left( \frac{dh}{dt} \right) = \frac{d(\ln h)}{dt} \quad (3)$$

In all the calculations, the depth was replaced by plastic depth as defined by Doerner and Nix.<sup>21</sup>

Poly Disperse Red 1 Acrylate (pDR1A) was purchased from Aldrich and used as received. For preparing the hydrogen-bonded complexes, poly(4-vinylpyridine) (p4VP, Polymer Source, Inc.,  $M_n = 5100 \text{ g mol}^{-1}$ ,  $M_w = 5400 \text{ g mol}^{-1}$ ) and Disperse Yellow 7 (DY7, Sigma-Aldrich, 95%) were dissolved in THF. After being stirred for 24 hours, the stock solutions were mixed to obtain the complexation degree of 0.5, indicating that, on average, every second repeat unit of the polymer is paired with a chromophore. This solution was then stirred 24 hours

before use. The formation of hydrogen bonding between the constituents has been confirmed by FTIR studies and this particular degree of complexation was chosen because it has previously been shown to be the most efficient for SRG formation.<sup>19</sup>

Films of pDR1A and p4VP(DY7)<sub>0.5</sub> were prepared by spin coating from THF onto silicon substrates. The films were annealed under vacuum for 12 h at 120 °C before use. The film thicknesses were measured using an Ambios XP200 surface profiler and were found to be 8 μm and 24 μm for pDR1A and P4VP(DY7)<sub>0.5</sub>, respectively. It has been reported<sup>18</sup> that the penetration depth of the nanoindenter should not exceed 30% of the film thickness in order to avoid substrate effects. Clearly our films are on the safe side of this limit. The indentation experiments were performed on a Hysitron Ubi3 indenter (Minneapolis, MN) with a load and displacement resolution of 0.1 mN and 0.2 nm, respectively. A blunted Berkovich diamond indenter tip (defect radius  $\cong$  850 nm) was used. The tip area function was calibrated on a fused quartz sample. Individual indents were separated from each other by at least 20 μm, several times the average indentation width. A peak indentation load of 500 μN was used for all indents with the loading rates of 500 μN s<sup>-1</sup>, 167 μN s<sup>-1</sup>, 50 μN s<sup>-1</sup>, 10 μN s<sup>-1</sup> and 5 μN s<sup>-1</sup>. A solid-state 532 nm (B & W Tek) laser was used to irradiate the samples with linearly polarized light using a power density of 15 mW cm<sup>-2</sup>.

Fig. 2a depicts a typical nanoindentation experiment in dark for both p4VP(DY7)<sub>0.5</sub> and pDR1A, when load and depth are recorded simultaneously. Generally, for any loading rate, it was

found that p4VP(DY7)<sub>0.5</sub> was slightly softer than pDR1A, evident in Fig. 2a from the larger penetration depth at maximum load for p4VP(DY7)<sub>0.5</sub> compared to pDR1A (the bulk glass-transition temperatures are comparable, 84 °C and 91 °C for p4VP(DY7)<sub>0.5</sub> and pDR1A, respectively). Fig. 2b shows the plastic depth calculated from the measured data and plotted against time both in dark and under 532 nm illumination. It is evident that when the loading rate is kept constant, the nanoindenter penetrates significantly deeper when the material is illuminated. Surprisingly, such light-induced softening is much more pronounced in the supramolecular p4VP(DY7)<sub>0.5</sub> complex than in the covalently functionalized pDR1A.

For calculating the strain-rate sensitivity, the stress and the strain-rate at the depth of 150 nm were determined. The load value for calculating indenter stress at 150 nm was taken from the linear regression of the load against depth curve between the depths 125 nm and 175 nm to avoid minor point-to-point variations in the data. The indentation strain rate (eqn (3)) was calculated over the 125–175 nm interval as the slope of regression in a plot of  $\ln(h)$  over time. The logarithms of the resulting stress-strain-rate data pairs for all loading rates are shown in Fig. 3 for both materials. The strain-rate sensitivities, obtained from the slopes from linear regression of these plots, for dark  $\rightarrow$  light are 0.021  $\rightarrow$  0.038 for pDR1A (an increase of 81%), and 0.086  $\rightarrow$  0.192 for p4VP(DY7)<sub>0.5</sub> (an increase of 123%). These strain-rate sensitivity increases for the polymers under light illumination, together with the data presented in Fig. 2, prove that (i) photoinduced softening takes place in both materials, (ii) for these illumination conditions the polymer-azobenzene complex is more light-sensitive than the conventional polymer, and (iii) the photosoftening effect depends on strain rate. For the last point, it should be noted that at high strain rates, p4VP(DY7)<sub>0.5</sub> has an observable difference for softening with light-on *versus* light-off (values of  $\log \sigma$  in Fig. 3) while pDR1A does not. For low strain rates, both materials have observable differences but p4VP(DY7)<sub>0.5</sub> photo-softens much more significantly than pDR1A. The fact that strain rate plays a role in the photo-softening process is a new finding and implies that whatever the mechanisms proposed to account for photo-softening, when tested with simulations, strain rate effects should be included. The strain rate dependence also has

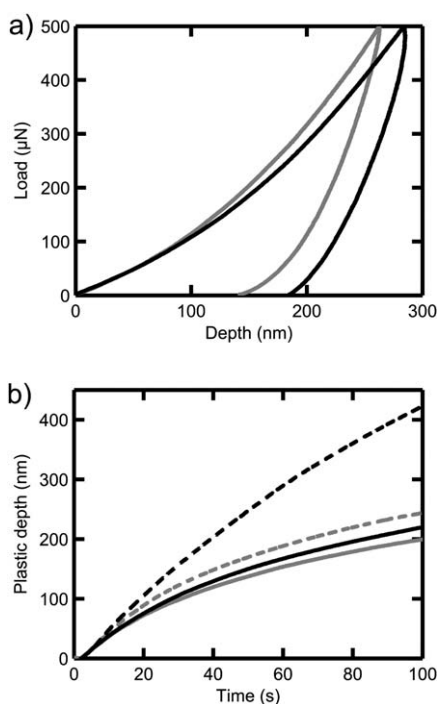


**Fig. 2** (a) The applied nanoindenter load as a function of depth and (b) the plastic depth as a function of time for loading rates of 5 μN s<sup>-1</sup>, for p4VP(DY7)<sub>0.5</sub> (black) and pDR1A (grey) under the illumination of 532 nm light (dashed line) and in darkness (solid line).

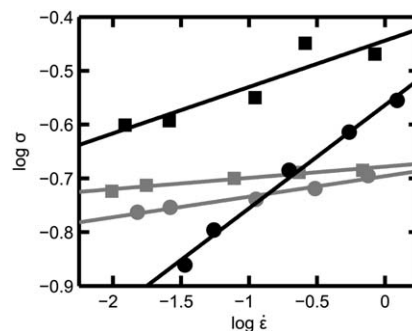


**Fig. 3** The stress-strain-rate data pairs at the depth of 150 nm for p4VP(DY7)<sub>0.5</sub> (black) and pDR1A (grey) under 532 nm light illumination (circle) and in darkness (squares).

implications on how these materials will be processed and used in the intended applications.

An interesting question is why the photosoftening is more pronounced for p4VP(DY7)<sub>0.5</sub> than for pDR1A. Both materials have proven efficient for SRG formation (which is why they were chosen for this study), but they are structurally and photochemically very different. Therefore they cannot be easily/directly compared, and their different photosoftening behaviour cannot be traced back to a single factor. The absorption coefficients of p4VP(DY7)<sub>0.5</sub> and pDR1A at the irradiation wavelength (532 nm) are *ca.*  $5.5 \times 10^3 \text{ cm}^{-1}$  and  $3.4 \times 10^4 \text{ cm}^{-1}$ , respectively. Hence we can estimate that at the depth of 150 nm (which was used for the strain rate sensitivity determination of Fig. 3), approximately 17% (p4VP(DY7)<sub>0.5</sub>) and 69% (pDR1A) of the incident irradiation is absorbed. This indicates that significantly less energy is required to cause a far bigger change in the case of p4VP(DY7)<sub>0.5</sub>, but on the other hand the actinic light penetrates much deeper, which itself may contribute positively to photosoftening.

There are two other factors that are likely to contribute to the more pronounced photosensitivity of the p4VP(DY7)<sub>0.5</sub>. Firstly, the intermolecular interactions between adjacent DR1 chromophores are probably more significant than between DY7 molecules due to the non-polar nature of the latter. Such interactions are likely to decrease the *cis*-azobenzene content at the photostationary state and may affect the rate of *trans*-*cis*-*trans* isomerization cycles of pDR1A. Hence the lower polarity, in combination with the lower molar concentration (50 mol%) of DY7 within the p4VP matrix may be favourable for efficient *trans*-*cis*-*trans* cycling. Second, there is no spacer between DY7 and P4VP whereas in pDR1A the azo unit is linked to the polymer backbone *via* an ethylene-spacer. This serves to keep the supramolecular complex amorphous despite the extended double azo rigid core, which tends to promote liquid crystallinity,<sup>22</sup> and may force the polymer to more efficiently accommodate the isomerization-induced chromophore movements. This may facilitate the photoinduced softening process compared to pDR1A, for which the azo units are kept apart from the polymer backbone by the short spacer.

The light-induced softening of azo-containing polymers is a unique characteristic and as this work demonstrates, non-covalent functionalization may provide a novel route towards materials with efficient photomechanical response. This observation, together with their facile preparation, suggests that supramolecular materials may exhibit significant potential in boosting the performance of azobenzene-based materials as, *e.g.*, nanostructuring tools, even if significantly more experimental work is required to comprehensively understand the structure–performance relationships that dictate the photosoftening effect. Nanoindentation provides a powerful measurement technique to quantify the connection between photoinduced changes in mechanical properties, including strain rate sensitivity, and photoinduced macroscopic movement of azo-polymer films, which is an important goal for both fundamental understanding on the unique properties of azo-polymers as well as their practical applicability. Our future work comprises more extensive research on the effect of the writing

wavelength and polarization, as well as the influence of the concentration and the nature of the photoactive unit on photosoftening.

## Acknowledgements

J. Vapaavuori acknowledges the financial support of the Finnish National Graduate School for Materials Physics, which enabled a 3-month visiting researcher appointment at McGill. We thank YaoYao Ding and Panu Hiekkataipale for instrument training, support, and helpful discussions, and Juho Hautala for measuring the absorption coefficients for p4VP(DY7)<sub>0.5</sub> and pDR1A films.

## Notes and references

- (a) P. Rochon, E. Batalla and A. Natansohn, *Appl. Phys. Lett.*, 1995, **66**, 136–138; (b) D. Y. Kim, S. K. Tripathy, L. Li and J. Kumar, *Appl. Phys. Lett.*, 1995, **66**, 1166–1168; (c) Z. Mahimwalla, K. G. Yager, J. Mamiya, A. Shishido, A. Priimagi and C. J. Barrett, *Polym. Bull.*, 2012, **69**, 967–1006.
- (a) B. Liu, M. Wang, Y. He and X. Wang, *Langmuir*, 2006, **22**, 7405–7410; (b) S.-I. Na, S.-S. Kim, J. Jo, S.-H. Oh, J. Kim and D.-Y. Kim, *Adv. Funct. Mater.*, 2008, **18**, 3956–3963.
- M. Haggui, M. Dridi, J. Plain, S. Marguet, H. Perez, G. C. Schatz, G. P. Wiederrecht, S. K. Gray and R. Bachelot, *ACS Nano*, 2012, **6**, 1299–1307.
- (a) A. Kravchenko, A. Shevchenko, V. Ovchinnikov, A. Priimagi and M. Kaivola, *Adv. Mater.*, 2011, **23**, 4174–4177; (b) S. Lee, H. S. Kang and J.-K. Park, *Adv. Mater.*, 2012, **24**, 2062–2062.
- (a) C. J. Barrett, A. L. Natansohn and P. L. Rochon, *J. Phys. Chem.*, 1996, **100**, 8836–8842; (b) T. G. Pedersen, P. M. Johansen, N. C. R. Holme, P. S. Ramanujam and S. Hvilsted, *Phys. Rev. Lett.*, 1998, **80**, 89–92; (c) J. Kumar, L. Li, X. L. Jiang, D. Y. Kim, T. S. Lee and S. Tripathy, *Appl. Phys. Lett.*, 1998, **72**, 2096–2098.
- (a) P. Lefin, C. Fiorini and J.-M. Nunzi, *Pure Appl. Opt.*, 1998, **7**, 71; (b) K. Sumaru, T. Yamanaka, T. Fukuda and H. Matsuda, *Appl. Phys. Lett.*, 1999, **75**, 1878–1880; (c) M. Saphiannikova, T. M. Geue, O. Henneberg, K. Morawetz and U. Pietsch, *J. Chem. Phys.*, 2004, **120**, 4039–4045; (d) M. L. Juan, J. R. M. Plain, R. Bachelot, P. Royer, S. K. Gray and G. P. Wiederrecht, *ACS Nano*, 2009, **3**, 1573–1579.
- K. G. Yager and C. J. Barrett, *J. Chem. Phys.*, 2004, **120**, 1089–1096.
- T. Sriksirin, A. Laschitsch, D. Neher and D. Johannsmann, *Appl. Phys. Lett.*, 2000, **77**, 963–965.
- N. Mechau, M. Saphiannikova and D. Neher, *Macromolecules*, 2005, **38**, 3894–3902.
- N. Mechau, D. Neher, V. Borger, H. Menzel and K. Urayama, *Appl. Phys. Lett.*, 2002, **81**, 4715–4717.
- (a) H.-K. Kim, X.-S. Wang, Y. Fujita, A. Sudo, H. Nishida, M. Fujii and T. Endo, *Macromol. Chem. Phys.*, 2005, **206**, 2106–2111; (b) A. Shimamura, A. Priimagi, J. Mamiya, T. Ikeda, Y. Yu, C. J. Barrett and A. Shishido, *ACS Appl. Mater. Interfaces*, 2011, **3**, 4190–4196.

- 12 P. Karageorgiev, D. Neher, B. Schulz, B. Stiller, U. Pietsch, M. Giersig and L. Brehmer, *Nat. Mater.*, 2005, **4**, 699–703.
- 13 (a) J. Gao, Y. He, F. Liu, X. Zhang, Z. Wang and X. Wang, *Chem. Mater.*, 2007, **19**, 3877–3881; (b) O. Kulikovska, L. M. Goldenberg and J. Stumpe, *Chem. Mater.*, 2007, **19**, 3343–3348; (c) N. Zettsu, T. Ogasawara, N. Mizoshita, S. Nagano and T. Seki, *Adv. Mater.*, 2008, **20**, 516–521; (d) Q. Zhang, X. Wang, C. J. Barrett and C. G. Bazuin, *Chem. Mater.*, 2009, **21**, 3216–3227; (e) A. Priimagi, G. Cavallo, A. Forni, M. Gorynsztejn-Leben, M. Kaivola, P. Metrangolo, R. Milani, A. Shishido, T. Pilati, G. Resnati and G. Terraneo, *Adv. Funct. Mater.*, 2012, **22**, 2572–2579.
- 14 M. R. Vanlandingham, J. S. Villarrubia, W. F. Guthrie and G. F. Meyers, *Macromol. Symp.*, 2001, **167**, 15–43.
- 15 M. L. Trunov, *J. Phys. D: Appl. Phys.*, 2008, **41**, 074011.
- 16 (a) Y. Lu, G. Tandon, D. Jones and G. Schoeppner, *Mech. Time-Depend. Mater.*, 2009, **13**, 245–260; (b) C.-C. Huang, M.-K. Wei and S. Lee, *Int. J. Plast.*, 2011, **27**, 1093–1102.
- 17 M. Moniruzzaman, P. Zioupos and G. F. Fernando, *Scr. Mater.*, 2006, **54**, 257–261.
- 18 A. Richter, M. Nowicki and B. Wolf, *Mol. Cryst. Liq. Cryst.*, 2008, **483**, 49–61.
- 19 (a) J. Vapaavuori, A. Priimagi and M. Kaivola, *J. Mater. Chem.*, 2010, **20**, 5260–5264; (b) J. E. Koskela, J. Vapaavuori, J. Hautala, A. Priimagi, C. F. J. Faul, M. Kaivola and R. H. A. Ras, *J. Phys. Chem. C*, 2012, **116**, 2363–2370.
- 20 M. J. Mayo and W. D. Nix, *Acta Metall. Mater.*, 1988, **36**, 2183–2192.
- 21 M. F. Doerner and W. D. Nix, *J. Mater. Res.*, 1986, **1**, 601–609.
- 22 C. Cojocariu and P. Rochon, *Macromolecules*, 2005, **38**, 9526–9538.